Experimental Demonstration of Real-Time Spectrum Analysis Using Dispersive Microstrip

Joshua D. Schwartz, *Student Member, IEEE*, José Azaña, *Member, IEEE*, and David V. Plant, *Senior Member, IEEE*

***Abstract*—We demonstrate the use of dispersive microstrip as a mechanism for obtaining the real-time Fourier transform of a time-limited signal within a predefined bandwidth. By etching a linearly-chirped impedance modulation into the upper plane strip-width, dispersive microstrip lines are created in which group-delay depends linearly on frequency within a prescribed bandwidth. When the group-delay satisfies a condition that is the temporal analog of the spatial Fraunhofer (far-field) condition of diffraction, the spectral components of an input signal are reordered in time such that the temporal envelope of the output signal corresponds to the Fourier-transform of the input. Experimental results are demonstrated for signals with frequency content from 4 to 8 GHz in a 1.2-ns window.**

***Index Terms*—Chirp transform, Fourier-transform (FT) processors, microstrip technology, quadratic-phase filter, real-time (RT) spectrum analysis.**

I. Introduction

REAL-TIME (RT) spectral analysis is a powerful signal processing tool with a myriad of interesting applications. The domain of RT Fourier transforms (RTFTs) has been explored over the years in many different kinds of media, ranging from the chirp-transform methods of surface acoustic wave filters [1] to zero-latency algorithms in digital processors dedicated to performing fast-Fourier transforms (FFTs) [2]. Particular interest has been generated in mapping the spectrum of a given input signal into the time-domain in RT, which would enable filtering, convolution, and correlation functions to be performed using time-domain processing. For example, it has been suggested that a signal of interest could be filtered in frequency by mapping it to its own FT in the time-domain, time-gating the segment corresponding to the desired frequencies, and then performing the inverse FT. Such frequency-to-time mapping has already been demonstrated in optical media using dispersive fiber gratings [3], [4]. Here, we present an experimental demonstration of an analogous mechanism for obtaining the RTFT of an electrical signal in microstrip technology.

Manuscript received July 28, 2005; revised Jan 11, 2006. This work was supported in part by the Natural Sciences and Engineering Research Council of Canada (NSERC) and by the Canadian Institute for Photonic Innovations (CIPI). The review of this letter was arranged by Associate Editor A. Weisshaar.

J. D. Schwartz and D. V. Plant are with the Photonics Systems Group, Department of Electrical and Computer Engineering, McGill University, Montréal, QC H3A 2A7, Canada (e-mail: joshs@photonics.ece.mcgill.ca).

J. Azaña is with the Institut National de la Recherche Scientifique-Énergie, Matériaux et Télécommunications, Montréal, QC H5A 1K6, Canada (e-mail: azana@emt.inrs.ca).

Digital Object Identifier 10.1109/LMWC.2006.872113

II. Theory of Dispersive Microstrips

The theory behind this demonstration was first proposed by Laso *et al.* [5], [6]. It is founded on the well-understood duality that exists between the equations governing the paraxial diffraction of an electromagnetic signal in space and those which govern the temporal dispersion of a narrow-band pulse. Both circumstances involve a similar set of approximations which yield parabolic differential equations [7]. In the context of a beam diffracting in space, monochromaticity of the beam is assumed, in addition to some narrow spatial confinement of the beam along an axis of propagation. This is commonly referred to as the paraxial approximation. Similarly, in the context of a pulse experiencing temporal dispersion, plane-waves are assumed (which are "monochromatic" in the spatial sense) and as pulses they are inherently band-limited. These complementary sets of approximations make both situations similar to diffusion equations, with the distinction that they both possess imaginary coefficients inherent to a propagating wave.

Arising from this duality, familiar concepts from imaging with conventional lenses find new applications when transposed from the spatial domain into the temporal domain. One such idea takes its cue from Fourier imaging. A paraxial beam subject to a spatial aperture function and diffraction will decompose spatially into its FT components in the far-field (Fraunhofer) regime.

In an analogous fashion, it has been proposed that an input signal $s_{\mathrm{i}}(t)$ constrained in time to Δt and incident on a device with a linear group delay will decompose into its FT components, ordered in time, if the following condition is satisfied [3] (corrected from the reference):

$$\left|\frac{\Delta t^2}{4\ddot{\Phi}_\nu}\right| < 1. \tag{1}$$

Here, $\ddot{\Phi}_\nu$ (ns/GHz) is the derivative of device group delay with respect to frequency (henceforth the "dispersion coefficient"). It has been shown [3] that the envelope of the resulting output $s_{\mathrm{o}}(t)$ is proportional to the FT of the input, scaled to the time domain by the dispersion coefficient

$$\hat{s}_o(t) \propto \left|FT\left(s_i(t)\right)\right|_{\upsilon=\frac{t}{\ddot{\Phi}_\nu}}. \tag{2}$$

In practice, this transformation is limited by the bandwidth of the realized dispersive device, which is a function of device chirp and length. Only frequency components within the designated band will be represented at the output. It should be noted

that this FT envelope exists on a chirped carrier frequency resulting from convolution with the dispersive device. As a result, the output is not a baseband representation of the FT, but has been upconverted by a linearly-varying frequency. This transformation was demonstrated originally in the optical domain [4] where dispersion was imparted by chirped fiber Bragg gratings. In the optical demonstration, the "carrier" frequencies modulating the FT are optical frequencies (∼200 THz), and the outputs were ∼0.1 ns in length (determined by the dispersion value and input bandwidth). Because the wavelength of the carrier is so short with respect to the dispersed signal's length, the envelope could be discriminated by the very process of signal photodetection.

The RTFT concept was extended for use on electrical signals in chirped microstrips [5]. In a linearly-chirped microstrip, the impedance of the microstrip is periodically modulated by strip-width modulation or an equivalent modulation in the microstrip ground plane. In this way, the local period varies linearly along the microstrip length. Such a microstrip couples the co- and counter-propagating quasi-TEM mode of an incident signal at the location along the strip where the local period corresponds to the input signal's frequency. If the condition of (1) is satisfied for a time-limited input signal, its spectral content will be linearly reordered in time upon reflection.

Whereas the previous work predicted signal behavior based on S-parameter measurements of a microstrip, here we present some examples of measured RTFTs produced by such a microstrip on various input signals, thus providing, to the best of the authors' knowledge, the first experimental demonstration of RTFT using microstrip technology.

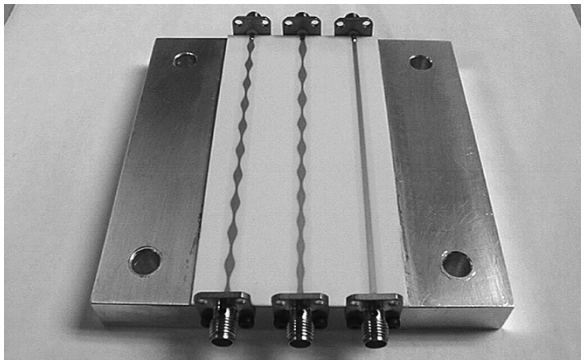

Fig. 1. Sample microstrips. The center microstrip is chirped for RTFT.

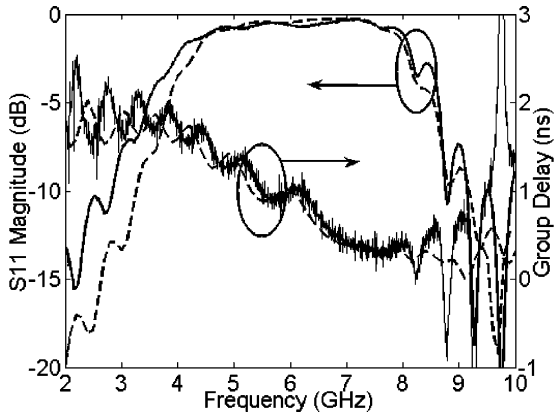

Fig. 2. Microstrip S_{11} and group delay, simulated (dash) and measured (solid).

III. Experimental Results

The microstrip was designed according to the equations laid out in [6]. The strip width modulation is chosen to vary the strip impedance around 50 Ω from $z = -L/2$ to $z = L/2$, according to the form

$$Z_o(z) = 50 \cdot \exp\left(A \cdot W(z) \cdot \sin\left(\frac{2\pi}{a_o} \cdot z + C \cdot \left(z^2 - \frac{L^2}{4}\right)\right)\right) \tag{3}$$

where "A" is dimensionless and fixes the maximum depth of modulation, "a_o" is the central period of the device, $W(z)$ is a tapering function (in this case, a Gaussian) which helps to suppress long-path Fabry–Perot type resonances due to abrupt impedance transitions at the ends of the device. "C" (m^{-2}) is the chirp, which is related to the dispersion coefficient by the effective permittivity ε_{eff} of the dielectric at 50 Ω

$$C = 4\pi \cdot \left(\frac{\sqrt{\varepsilon_{eff}|_{50\ \Omega}}}{c}\right)^2 \cdot \frac{1}{\ddot{\Phi}_\nu}. \tag{4}$$

The general form of the impedance modulation is $\exp(\sin(\omega_o \cdot z))$ because it offers the benefits of smooth and continuous impedance variation (which reduces parasitic effects), while at the same time suppressing the harmonic resonances that would occur with a simple sinusoid. The integration constant of $-C(L^2/4)$ ensures that at each extreme of the structure $(z = \pm L/2)$ the impedance is 50 Ω provided that L is an integer multiple of a_o.

The authors' design targeted an operating bandwidth of 4 GHz with a center frequency of 6 GHz. The microstrip was 10 cm in length and was fabricated on a 1.27-mm alumina substrate ($\varepsilon_r = 9.41$, $\tan\delta = 0.0007$ at 10 GHz) with gold-alloy metallization ($\sigma \sim 4 \cdot 10^7$ S/m). The strip was mounted on an aluminum baseplate and connectorized to SMA cables (Fig. 1). The final length of the structure was 10 cm and had a chirp of $C = -2600\ \text{m}^{-2}$, which corresponds to a dispersion coefficient of $\ddot{\Phi}_\nu = -0.38$ ns/GHz. Thus, the Fraunhofer condition of (1) was satisfied for signals within a time window of $\Delta t < 1.2$ ns. This would yield a time-bandwidth product of approximately five, however, the authors will stress that time-bandwidth products exceeding ten are quite feasible.

Shown in Fig. 2 are the simulated and measured S_{11} and group delay results for the microstrip, obtained, respectively, by Agilent's Momentum software and a vector network analyzer. The group delay features oscillations as a result of end-to-end resonances which were not completely eliminated by the applied tapering technique. These oscillations are somewhat more noticeable in this letter than in the previous work [5] due to the structure's smaller bandwidth and overall size, however, their effect on the overall performance is small. The simulations also did not include the connectorization of the device to SMA-type

connectors as these connections were hand-soldered and would not be present in an integrated microstrip.

In order to test the performance of the microstrip, a broadband 6-dB directional coupler was used to isolate the reflected response. In future designs, such a coupler could readily be integrated with the microstrip itself. The other end of the microstrip was 50-Ω terminated. Input signals were generated by a high-speed pulse-pattern generator and patterns were chosen to contain frequency peaks and nulls within the frequency band of interest. Using a temporal window of 0.6 ns to easily satisfy (1), data patterns of up to 6 b at frequencies of 10 and 12 Gbps (yielding spectral peaks around 5 and 6 GHz) were applied as inputs surrounded by strings of zeros to effect a time window. It should be noted that although the microstrip was tested here with digital bit-signaling, it is in no way limited to such signals. They were employed for ease of time-windowing.

For each input, the microstrip yielded a time-domain output approximately 1.5 ns in length (recall that $\ddot{\Phi}_\nu = 0.38$ ns/GHz over a designed bandwidth of 4 GHz). The signal contained the FT information modulated on a chirped-sinusoidal carrier frequency which varied from 4 to 8 GHz. The FT information was then extracted by peak-detection of the output signal. The method of peak detection is inherently limited in resolution, particularly at the lower frequencies where there are only a few peaks present, however, it represents a simple and easily implemented RT mechanism whose resolution would improve at higher frequencies of operation. Some RT alternatives to using peak detection here include mixing the signal against a frequency sweep to down-convert the response to baseband, or else measuring the signal average power over time.

Experimental measurements were recorded using a digital sampling oscilloscope. Results for several 6-b sequences are presented in Fig. 3 and are compared to measurements taken using a conventional spectrum analyzer by scaling the time-domain detected response to the corresponding frequency range using the known dispersion coefficient of the device and the simple transformation $\nu = t/\ddot{\Phi}_\nu$. Since the device chirp was negative, lower frequencies were reflected first by the microstrip and so form the leading edge of the temporal signal, thus the signal has been reversed in time to properly display the results. The microstrip compares favorably to results obtained from a spectrum analyzer, with some slight deviation near the frequency extremes due to end-connector effects, which would not exist in an integrated microstrip circuit.

IV. Conclusion

In this letter, we have experimentally demonstrated a RT analog mechanism for obtaining the FT of a time-limited signal. Some limitations of this technique include narrow time-windows of operation and relatively long microstrip lengths.

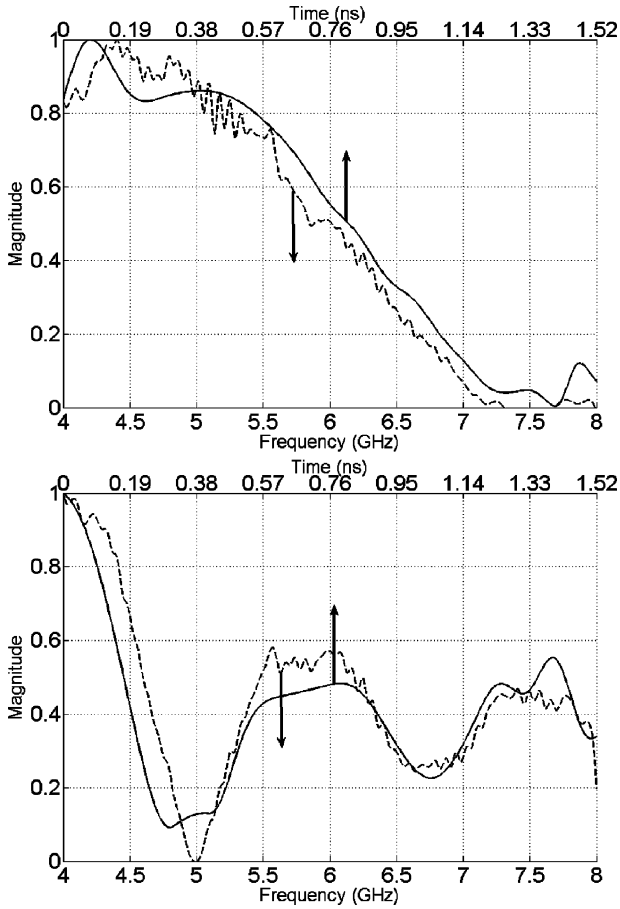

Fig. 3. Experimentally measured RTFTs. The spectra of 6-b signals "010 100" (top) and "100 111" (bottom) were measured using a spectrum analyzer (dashed, frequency domain) and a peak-detected dispersive microstrip (solid, time-domain). Results have been normalized in magnitude for clarity.

Acknowledgment

The authors wish to thank R. Morawski and Dr. T. Le-Ngoc, for their experimental assistance.

References

[1] M. A. Jack, "Fast-Fourier-transform processor using SAW chirp filters," *Electron. Lett.*, vol. 14, pp. 634–635, Sep. 1978.

[2] E. Cetin, R. C. S. Morling, and I. Kale, "An extensible complex fast Fourier transform processor chip for real time spectrum analysis and measurement," *IEEE Trans. Instrum. Meas.*, vol. 47, no. 1, pp. 95–99, Feb. 1998.

[3] J. Azaña and M. A. Muriel, "Real-time optical spectrum analysis based on the time-space duality in chirped fiber gratings," *IEEE J. Quant. Electron*, vol. 36, no. 5, pp. 517–526, May 2000.

[4] J. Azaña, L. R. Chen, M. A. Muriel, and P. W. E. Smith, "Experimental demonstration of real-time Fourier transformation using linearly chirped fiber bragg gratings," *Electron. Lett.*, vol. 35, pp. 2223–2224, Dec. 1999.

[5] M. A. G. Laso, T. Lopetegi, M. J. Erro, D. Benito, M. J. Garde, M. A. Muriel, M. Sorolla, and M. Guglielmi, "Real-time spectrum analysis in microstrip technology," *IEEE Trans. Microw. Theory Tech.*, vol. 51, no. 3, pp. 705–717, Mar. 2003.

[6] ——, "Chirped delay lines in microstrip technology," *IEEE Microw. Wireless Compon. Lett.*, vol. 11, no. 12, pp. 486–488, Dec. 2001.

[7] B. H. Kolner, "Space-time duality and the theory of temporal imaging," *IEEE J. Quant. Electron.*, vol. 30, no. 8, pp. 1951–1963, Aug. 1994.